5
Microbial Laser Light Scattering

STEPHEN E. HARDING

Department of Applied Biochemistry and Food Science, University of Nottingham, Sutton Bonington, Leicestershire LE12 5RD, UK

Introduction

Microbes will scatter light: that is to say, they will absorb and re-emit visible light scattering the light in all directions. The way the intensity of the scattered light from a population of microbes in a solution or suspension – or in some cases from just a single microbe – varies with angle can give us useful information concerning microbial structure: this type of measurement is called either 'total intensity light scattering', 'differential light scattering', 'classical light scattering' or, as seems to be more favoured now 'static light scattering'. A different type of light scattering measurement is when rapid intensity fluctuations caused by Brownian movement (or any inherent motility) of the microbes are studied: this needs monochromatic incident radiation of high coherence – i.e., from a laser – and is known as 'quasi-elastic light scattering' or now more popularly as 'dynamic light scattering'. This type of measurement can also yield valuable information on microbial structure as well as dynamic properties, such as head-tail association kinetics of T-even bacteriophage viruses or the physical changes occurring within bacterial spores during germination. Although lasers are not essential for static light scattering, they are still widely used for such because of their high intensity and monochromaticity, as well as being highly focussed.

Detailed reviews have appeared before on the theory and practice of both static light scattering applied to bacteria (Wyatt, 1973) and dynamic light scattering applied to viruses and bacterial motility (Bloomfield, 1981; Bloomfield and Lim, 1978). A further review appeared later from the present author (Harding, 1986) which included the use of turbidity measurements using high quality spectrophotometers. The purpose of this present article is to review our own experience of laser methods in its application to microbial systems. In particular, it is hoped our views on the importance of not relying on a single light scattering technique but, where possible, combining laser light scattering observations with other independent measurements (such as sedimentation analysis in the analytical ultracentrifuge for virus studies, or electron microscopic studies in the case of studies on microorganisms) will be noted.

Biotechnology and Genetic Engineering Reviews – Vol. 14, April 1997
0264-8725/97/14/145-164 $20.00 + $0.00

PECULIARITIES OF STUDYING WHOLE MICROORGANISMS

Studies on intact microbes offer certain advantages and certain disadvantages as far as laser light scattering techniques are concerned. The advantages include (1) the greater signal to noise ratio (that is to say also the so-called 'dust problem' is not as severe (see, for example, Sanders and Cannell, 1980); (2) the correspondingly smaller concentrations generally required to give a sufficient signal; (3) since the wavelength of the incident laser light can be of the same order as the maximum dimension of the microbe (~1μm), internal structural information can in principle be obtained from the nature of the 'resonances' in the angular scattered intensity envelopes (Wyatt, 1973).

The relatively large size – compared to macromolecular systems – of microbial scatterers also brings problems, namely that we are on the limits – and in many cases go beyond them – of the applicability of the relatively simple 'Rayleigh-Gans-Debye' representations of the scattering data. The criteria for these representations are summarised by the two equations (see for example Wyatt, 1992):

$$|(n/n_o) - 1| << 1 \tag{1}$$

$$|(4\pi n_o a/\lambda_o)\,(n/n_o)| << 1 \tag{2}$$

a is the maximum dimension of the scatterer, n, n_o the refractive indices of the scatterer and surrounding medium respectively and λ_o the (vacuo) wavelength of the incident light (the corresponding value for the wavelength through the surrounding medium is thus λ_o/n_o). These criteria are usually satisfied for smaller microbes, such as most viruses, and the highly useful limiting case or 'Zimm plot' can also be applied. They can also be satisfied for larger microorganisms – for example vegetative bacterial cells suspended in an aqueous media where $|n\text{-}n_o|$ is very small – although because of the resonances, the Zimm plot and related representations become inapplicable. For the highly dehydrated and refractile bacterial spores – particularly air-borne particles – the criteria are not satisfied, and for this case interpretation of the scattering records can be rendered opaque because of the complexity of the mathematical representations ('Mie'-theory – or in full 'Lorenz-Mie' theory (Wyatt, 1973)) involved (Kerker, 1969). A further problem for the larger or denser microbes is that sedimentation (i.e., settling under gravity) phenomena can also obscure this interpretation. Allowing for these reservations, nonetheless laser light scattering methods – both static and dynamic – can provide powerful non-destructive probes into the structure and dynamics of microbial systems.

The purpose of this review is, therefore, to give the interested reader an appreciation of some of the applications of laser light scattering to specific microbiological systems: first of all we consider virus systems, and then the larger systems of bacteria and other cellular microorganisms. In the interests of not concealing the wood from the trees this review is not, however, meant to be a treatise in physics. Only a skeleton of theory is given: details of the theory and experimental detail can be found in for example Kerker's (1969) book and articles by Wyatt (1973) and Ludlow and Kaye (1979) for what is now popularly called 'static' light scattering, in a book by Schmitz (1990), a comprehensive edited book by Brown (1993) and a review by Bloomfield (1981) for dynamic light scattering. Burchard (1992) gives a detailed consideration of both dynamic and static light scattering within the Rayleigh-Gans-Debye limit. A much more elementary consideration of methodology and instrumentation, written for an audience of molecular

biologists, has been given by two other articles of the author's: Harding (1994a) for static light scattering and Harding (1994b) for dynamic light scattering. We would also like to stress the importance of combining light scattering measurements, wherever possible, with other independent measurements of structure and morphology wherever possible – for example ultracentrifugal analysis for viral systems or electron microscopical analysis of bacteria – before rigorous conclusions are drawn. In some of the examples we quote, the usefulness of this sort of combination is illustrated.

Applications to viruses

STATIC LIGHT SCATTERING

This provides us with information about the molecular weight and conformation of virus systems. For smaller microbes, like many viruses, the simpler Rayleigh-Gans-Debye (RGD) theory is applicable. Another useful criterion is usually satisfied: that is the product of the 'Bragg wave vector' q (cm^{-1}) (sometimes given the symbol k or K) times the 'radius of gyration' R_g (cm) is very small. That is to say:

$$q.R_g << 1 \tag{3}$$

where $q=(4\pi n_o/\lambda_o)\sin(\theta/2)$ and is thus a function of angle θ for a given incident (vacuo) wavelength λ_o, and R_g is the 'root mean square distance of the mass elements of a particle from the centre of mass' – i.e., the mass distribution which is a function of the particle conformation. If this criterion is satisfied, together with the criteria of eqns (1) and (2) it is possible to use the 'static Zimm plot' to obtain (1) the (weight average) molecular weight, M_w, (2) the radius of gyration, R_g and (3) the thermodynamic second virial coefficient, B (or A_2). The static Zimm plot is based on the following relation:

$$Kc/R_\theta = [1/P(\theta)].[(1/M_w)(1 + 2BM_w c)] \tag{4}$$

where the assumption is made that one non-ideality term, B, is sufficient (usually reasonable for dilute solutions). c is the particle concentration (g/ml), K is an experimental constant which includes the square of the refractive index increment, dn/dc which depends largely on the relative amounts of protein and nucleic acid: in the extremes of pure protein and pure nucleic acid, dn/dc has the extremes of ~0.19 ml/g and ~0.16 ml/g for scattering of light in the visible region. R_θ is what light scatterers call the 'Rayleigh excess ratio' which is a measure of the ratio of the intensity of the scattered light i_θ at a scattering angle θ to the incident light intensity I (n.b., if unpolarised light is used – e.g., from a non-laser light source – an extra term is needed). $P(\theta)$ is the 'form factor, which in the limit of the scattering angle, $\theta > 0$ takes the form:

$$P(\theta) = 1 - (16n_o^2/3\lambda_o^2)R_g^2.\sin^2(\theta/2) \tag{5}$$

The static Zimm plot involves plotting $Kc/R\theta$ versus $\sin^2(\theta/2) + kc$, where k is an arbitrarily (positive or negative) constant chosen to conveniently space out the data points. The data points are extrapolated two ways: one to zero angle, the other to zero concentration. The zero angle and zero concentration lines are themselves extrapolated to zero concentration and zero angle respectively: the (limiting) slope of the zero angle line allows the calculation of B from the slope; the (limiting) slope of the zero

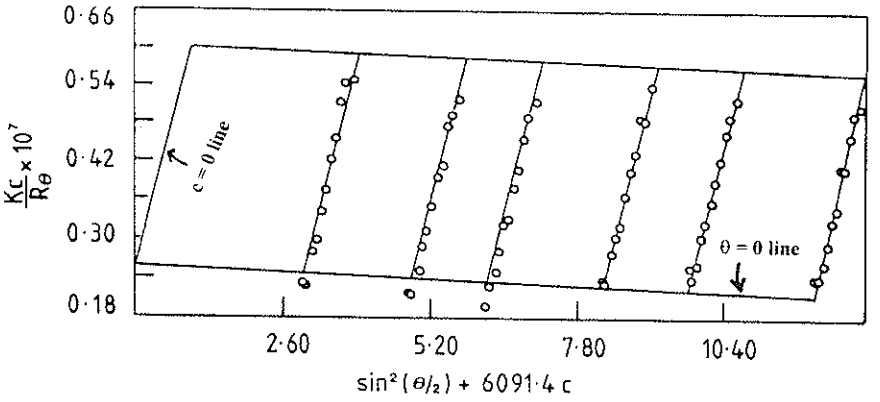

Figure 1. Static Zimm plot for tobacco mosaic virus. In a solvent of ionic strength 0.006M and pH 7.5. M_w from common intercept ~ 40×10^6 Da. The slope of the θ=0 line is negative indicating a negative B, symptomatic of possible self-association effects. (Adapted from Johnson and Brown, 1992.)

concentration line permits the calculation of R_g, and the common intercept on the ordinate = $1/M_w$. An example of this 'biaxial' extrapolation procedure in the static Zimm plot for tobacco mosaic virus, TMV (M_w~40×10^6), is given in *Figure 1* (Johnson and Brown, 1992). An earlier determination for TMV was given by Boedtker and Simmons (1958). Another good example can be found for R17 virus (M_w~4×10^6) (Camerini-Otero, 1973). For very large viruses such as *Vaccinia* virus (M_w~3×10^9) (Fiel *et al.*, 1970) the Zimm plot shows curvature which can be largely removed by using a modified form of Zimm plot called a 'Guinier' (see, e.g., Burchard, 1992) plot in which the ordinate axis is plotted as log (Kc/R_θ).

USE OF R_G AND B FOR VIRAL CONFORMATION ANALYSIS

The radius of gyration from the Zimm or modified Zimm (Guinier) plots, can – particularly if used in combination with other hydrodynamic parameters such as the translational diffusion coefficient (see below), sedimentation coefficient, intrinsic viscosity or rotational diffusion based parameters – be used to model the conformation of a virus in terms of sophisticated bead models using computer programmes such as SOLPRO which now permit such modelling without the worry of assigning a value for the degree of hydration of the assembly (Garcia de la Torre *et al.*, 1997). Alternatively, a graphical-based programme called ELLIPS3 permits the triaxial shape of the particle to be uniquely assigned by a simple combination of R_g with B and the intrinsic viscosity [η] (ml/g) (Harding *et al.*, 1997). Finally, if a specific conformation of the virus is assumed (e.g., a rod), alternative relations (Kerker, 1969) for P(θ) are available permitting for example mass per unit length M_L determinations and persistence length, a, estimations, highly useful for representing the flexibility of linear virus particles (a has limiting values of 0 for a completely flexible coil to infinity for a perfectly rigid rod). A good example of this, using a 'master curve' procedure to the extracellular rod-shaped microbial polysaccharide xanthan has been recently given by Berth *et al.*, (1996), with M_L ~ 2000 Da nm^{-1} and a = 150nm.

DYNAMIC LIGHT SCATTERING

Dynamic light scattering contributions – in terms of the translational diffusion coefficient, D – to virology have been in four principal areas: (1) hydrodynamic rigid-bead modelling; (2) flexible particle modelling; (3) molecular weight measurement; and (4) following the dynamics of assembly or swelling processes. As we have just mentioned, hydrodynamic modelling procedures based on dynamic light scattering measurements are now well established (Bloomfield, 1981; Garcia de la Torre, 1989; Garcia de la Torre *et al.*, 1997) as well as data capture and analysis protocols (Bloomfield and Lim, 1978).

Dynamic light scattering is different from static in the sense that the technique is based on fluctuations in intensity caused by the Doppler type of broadening of the monochromatic incident wavelength from the Brownian (or other types of movement such as cellular motility) motions of the scattering particles. These fluctuations are recorded in terms of the decay of an autocorrelation function with time (for microbes usually in the μs-ms time range): the faster the fluctuations, the more rapid the decay and the greater the diffusional mobility.

For quasi-spherical viruses such as turnip yellow mosaic virus (TYMV), tomato bushy stunt virus (TBSV) and many other plant viruses, a simple single exponential term correlation equation, in terms of the normalised intensity autocorrelation function, $g^{(2)}(\tau)$ = where τ is the delay time – is usually adequate (Pusey, 1974) provided that heterogeneity is not significant:

$$g^{(2)}(\tau) - 1 = \exp(-Dq^2\tau) \tag{6}$$

where q, as previous, is the Bragg wave vector. The translational diffusion coefficient, D, can thus be readily obtained from a plot of ln $[g^{(2)}(\tau) - 1]$ versus τ (*Figure 2a*). Measurements based on a single angle – usually 90° to minimise dust problems – are usually sufficient. If the system is polydisperse, D obtained from eqn 6 will be a 'z-average', and a measure of the polydispersity is usually given in the form of a 'polydispersity factor', PF, which is formally defined as the normalized z-average variance of the distribution of diffusion coefficients (see, e.g., Pusey, 1974). The D value obtained from eqn 6 is usually, for comparison purposes, corrected to standard conditions of solvent temperature and viscosity, η, namely a temperature of 20°C and the viscosity of water at 20°C via the relation (van Holde, 1985):

$$D_{20,w} = [(293.15/T).(\eta/\eta_{20,w})].D \tag{7}$$

By analogy with static light scattering, the $D_{20,w}$ value is then normally corrected for non-ideality (exclusion volume and polyelectrolyte) by measurement at several concentrations and extrapolation to zero concentration to give a parameter, $D^{\circ}_{20,w}$, free of these effects (Tanford, 1961). As with the case for macromolecules, for viruses a linear extrapolation is usually adequate (*Figure 2b*):

$$D_{20,w} = D^{\circ}_{20,w}(1 + k_d c) \tag{8}$$

where k_d is the concentration dependence diffusion parameter defined by (Harding and Johnson, 1985a):

$$k_d = 2BM - k_s - v \tag{9}$$

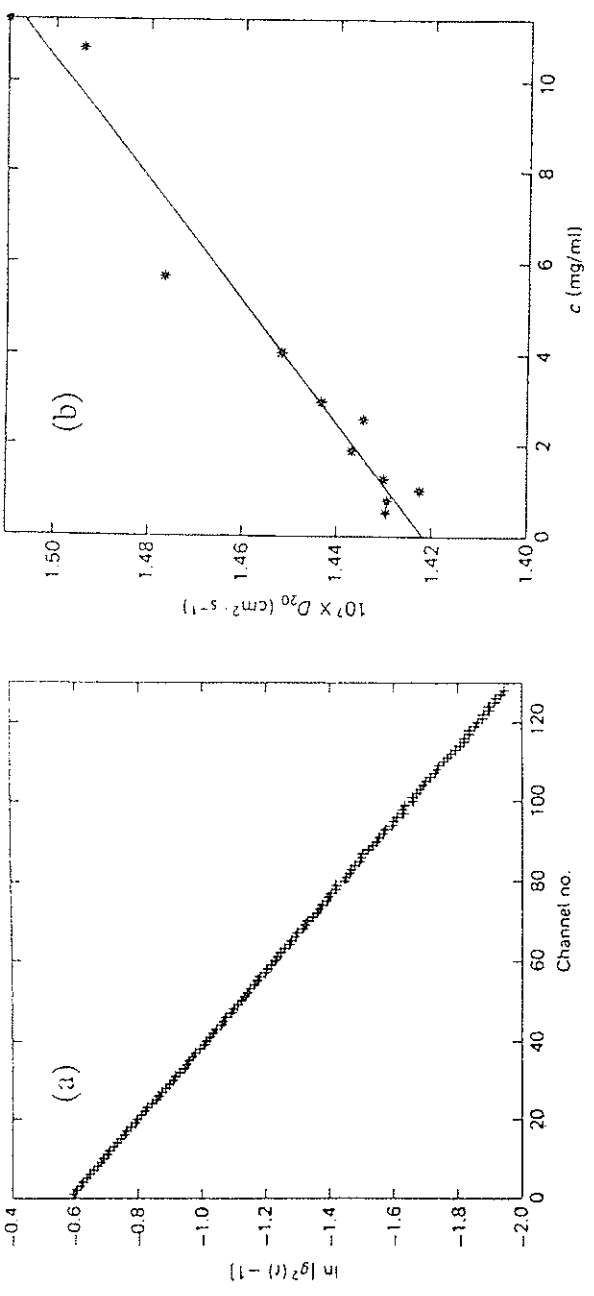

Figure 2. Dynamic light scattering analysis for a quasi-spherical virus (TYMV). (a) Linear normalised autocorrelation decay plot. Channel number = delay time (τ)/sample time (τ_s). τ_s = 1.0μs; experimental duration time = 60s; scattering angle θ = 90°; temperature = 24.85°C; concentration c = 4.1 mg/ml; (b) Linear extrapolation of the apparent (i.e. measured at a finite concentration) diffusion coefficient to zero concentration for TYMV. (From Harding and Johnson, 1985b.)

k_s is the corresponding sedimentation or 'translational frictional coefficient' concentration dependence parameter and $\bar{v}$ the partial specific volume (a parameter analagous to the refractive index increment, dn/dc and usually between 0.6 – 0.73 ml/g for a virus depending on its proportion of nucleic acid to protein). This equation, with the opposing effects of the second thermodynamic virial coefficient, B, and k_s, explains why the concentration dependence of the translational diffusion coefficient is usually not as severe compared with some other hydrodynamic parameters such as the sedimentation coefficient. Furthermore if k_s is known from sedimentation velocity experiments in the analytical ultracentrifuge, eqn 8 and eqn 9 provide an alternative route to eqn 4 for obtaining B, which as we have mentioned can be a useful parameter for viral shape determination in solution.

DYNAMIC LIGHT SCATTERING AND VIRAL SIZE, SHAPE AND FLEXIBILITY

A simple relation, the Stokes-Einstein relation, exists between D (or $D^{\circ}_{20,w}$) and the radius (known as the 'Stokes radius' or 'hydrodynamic radius') of the equivalent sphere, r_H:

$$r_H = (k_B T)/(6\pi\eta_{20,w} D^{\circ}_{20,w}) \tag{10}$$

with k_B the Boltzmann's constant, T = 293.15K, and $\eta_{20,w}$ the corresponding viscosity of water. Dynamic light scattering has been used in this way, for example to compare the gross morphology of TBSV variants (Molina-Garcia *et al.*, 1990) and TYMV in various aqueous solvents (Harding and Johnson, 1985b).

For general shapes the equivalent relation is in terms of the translational frictional coefficient, *f*:

$$D^{\circ}_{20,w} = (293.15R)/(N_A f) \tag{11}$$

(where R is the gas constant and N_A Avogadro's number) and *f* can be modelled in terms of the shape or the hydration of the particle (see, e.g., Tanford, 1961; Harding, 1995) either in terms of ellipsoids or in terms of bead models: excellent examples of the latter can be found for the T-even bacteriophages (see Garcia de la Torre, 1989 and references therein).

By combining eqn (11) with an equivalent expression for the sedimentation coefficient, the frictional coefficient *f* is removed resulting in the Svedberg equation (Svedberg and Pedersen, 1940; see also van Holde, 1985) for molecular weight:

$$M = (s^{\circ}_{20,w}/D^{\circ}_{20,w}).[(293.15R)/(1-\bar{v}\,\rho_{20,w})] \tag{12}$$

where $\rho_{20,w}$ is the density of water at 20°C. Equivalent expressions to eqns (10–12) can of course be used for different reference temperatures. Dynamic light scattering translational diffusion coefficient determinations have also been used via the Svedberg equation to evaluate for example the molecular weights of the bacteriophages type 5 adenovirus (Oliver *et al.*, 1976), MS2 (Nieuwenhuysen and Clauwaert, 1978), VS11 (Sakaki *et al.*, 1979), and also infectious pancreatic necrosis virus (Dobos *et al.*, 1977).

For rod-shape and other non-spheroidal viruses it is necessary to correct for rotational diffusion effects by measurements at several angles followed by a subse-

quent extrapolation to zero angle: a procedure which has yielded both D and the rotational diffusion coefficient D_R for tobacco mosaic virus (TMV) (Johnson and Brown, 1992) and the bacteriophages T4B and T7 (Hopman *et al.*, 1980). D and D_R values have also been obtained at a single angle (90°) from bimodal resolution using the 'SIPP' algorithm (Timachenko *et al.*, 1990). Both extrapolations of D and D_R can now be performed in a biaxial 'Dynamic Zimm plot' by analogy with the the 'Static Zimm plot' (Burchard, 1992) and this procedure has been applied to microbial polysaccharides (Burchard, 1992; Harding *et al.*, 1996) where the spheroidal approximation is inapplicable. For rod-shape viruses anisotropy of the translational D itself can be a problem (Wilcoxon and Schurr, 1983). A further complication is one of particle flexibility, and Fujime and Maeda (1985) have considered this for filamentous fd bacteriophage by model fitting the apparent D (in this instance this means at a finite angle θ or wave vector q) as a function of q and obtained a value for the persistence length a of (2000±200) nm consistent with a weakly bending rod. Song *et al.* (1991) reached virtually exactly the same conclusion for the related M13 virus, and obtained a persistence length a = (2200±200) nm.

COMPARISON OF DATA FROM STATIC AND DYNAMIC LIGHT SCATTERING WITH OTHER HYDRODYNAMIC DATA.

The dangers – largely because of the serious errors resulting from even trace amounts of dust and other contaminating material – of using light scattering techniques in isolation for the characterisation of *macromolecular* solutions are widely appreciated (Sanders and Cannell, 1980; Godfrey *et al.*, 1982). For solutions of *viruses* the situation is not as severe compared to the situation encountered when studying smaller molecules and assemblies, but independent confirmatory or complementary measurements – from for example analytical ultracentrifugation or electron microscopy – are always useful. In general, agreement is good. Johnson and Brown (1992) discussed the excellent agreement molecular weight measurements from the dynamic light scattering/Svedberg equation ($M \sim 40.8 \times 10^6$) with that from chemical analysis (39.4×10^6) and sedimentation equilibrium (41.6×10^6) for TMV. The result is also consistent with the value of $\sim 40 \times 10^6$ from their static Zimm plot (see *Figure 1*).

Another good example of agreement of results from laser light scattering with independent techniques is for the case of the quasi-spherical TYMV (Harding and Johnson, 1985b): the molecular weights evaluated from the translational diffusion coefficient and sedimentation coefficient via the Svedberg equation for four different solvents are in excellent agreement with those obtained independently from sedimentation equilibrium (*Table 1a*). Furthermore, values for the second viral coefficient from combination of the coefficient k_d obtained from the concentration dependence of the diffusion coefficient and k_s, the corresponding parameter from sedimentation velocity, are in excellent agreement with the virial coefficient obtained from sedimentation equilibrium (*Table 1b*). The hydrodynamic radii calculated from the translational diffusion coefficient are also in excellent agreement with the 'thermodynamic' radii from the second thermodynamic virial coefficient from sedimentation equilibrium (*Table 1c*).

Despite their large size, it is possible to obtain preparations of virus solutions with very high monodispersities. This has made them highly suitable systems for testing

Table 1. Physical data for Turnip Yellow Mosaic Virus (TYMV).

(a) Molecular Weight

pH	I[a]	$10^{-6} \times M_w$[b] (±0.05) g/mol	$10^{-6} \times M_w$[c] (±0.2) g/mol	$10^{-6} \times M_w$[d] (±0.2) g/mol
7.8	0.1	5.80	5.5	5.3
6.8	0.1	5.73	5.8	5.5
6.0	0.1	5.75	5.6	5.6
4.75	0.1	5.77	5.6	5.6
6.8	0.2	5.64	5.7	5.5

(b) Thermodynamic ("osmotic pressure") second virial coefficient, B

pH	I[a]	$10^{4} \times B$[e] (±0.10) ml.mol.g^{-2}	$10^{4} \times B$[f] (±0.4) ml.mol.g^{-2}
7.8	0.1	1.30	1.3
6.8	0.1	1.21	1.5
6.0	0.1	1.25	1.3
4.75	0.1	1.10	1.3
6.8	0.2	1.32	1.7

(c) Radii of equivalent spherical particle

pH	I[a]	r_H[g] (±0.2) nm	r_B[h] (±0.5) nm
7.8	0.1	15.1	16.3
6.8	0.1	15.1	15.8
6.0	0.1	15.2	15.9
4.75	0.1	15.5	15.4
6.8	0.2	14.9	16.1

Agreement between results from dynamic light scattering combined with sedimentation velocity in the ultracentrifuge with sedimentation equilibrium studies.

[a]ionic strength; [b]from the sedimentation coefficient and the translational diffusion coefficient via the Svedberg equation; [c]whole distribution weight average from sedimentation equilibrium; [d]point weight average extrapolated to zero concentration (sedimentation equilibrium); [e]from k_s and k_c; [f]from sedimentation equilibrium; [g]from the dynamic light scattering translational diffusion coefficient; [h]from the (sedimentation equilibrium) value for B. (From Harding and Johnson, 1985b.)

experimentally the validity of theories representing the concentration dependence of the translational diffusion coefficient and related hydrodynamic parameters (Harding and Johnson, 1985a,b).

ANALYSIS OF DYNAMICS OF VIRUS SYSTEMS

Arguably the greatest value of laser light scattering methods – particularly dynamic light scattering – in virology is for the analysis of the dynamics of self-assembly and related processes. We quote just two examples here. One (see, e.g., *Figure 3a*) is the analysis of the kinetics of head/tail assembly reactions for bacteriophages (Baran and Bloomfield, 1978; Welch and Bloomfield, 1978; Benbasat and Bloomfield, 1975, 1981; Chernyak, 1982). The second (*Figure 3b*) is the analysis of the effects of the removal of calcium ions on the dynamics of swelling of southern bean mosaic virus (SBMV), monitored by hydrodynamic diameters and polydispersity factors from dynamic light scattering, in conjunction with total intensity measurements (Brisco *et al.*, 1986).

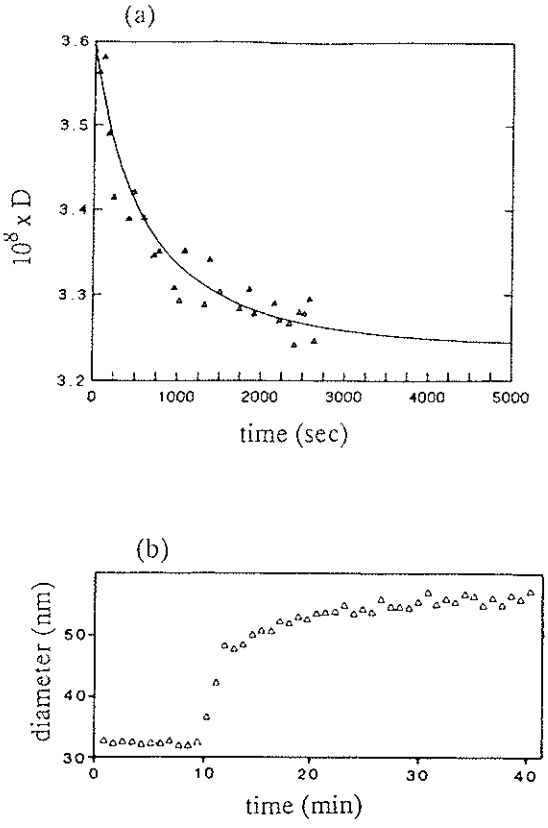

Figure 3. Following the dynamics of viral processes using dynamic light scattering. (a) Head-tail association kinetics of T4D bacteriophage. Line fitted corresponds to an association rate constant, k = 7.9 × 10^{-9} $M^{-1}s^{-1}$. (From Benbasat and Bloomfield, 1981.); (b) Swelling of southern bean mosaic virus on removal of Ca^{++} ions. (From Brisco *et al.*, 1985.)

Applications to bacterial and other cellular microbial systems

Both static and dynamic laser light scattering have provided major inroads into our understanding of bacterial systems; perhaps most widely known is the application of dynamic light scattering as a probe into the motility of bacteria and protozoa. However there has also been progress in other areas, such as (1) the use of static light scattering for modelling the structure in terms of refractive index profiling – of isolated quasi-spherical bacterial spores and isolated marine microorganisms, and also (2) in the application of dynamic light scattering for following the dynamics of suspensions of bacterial spore ensembles as a probe into their high resistance to thermal destruction; we will now survey some aspects of the progress in all these general areas.

STATIC LIGHT SCATTERING

With the larger microbes resonances in the angular scattered intensity profiles become significant – even at lower angles – and the static Zimm plot and related methods become

inapplicable. One ingenious solution was that of Morris *et al.* (1974) who increased the wavelength of the incident radiation to the infra-red, allowing application of the Zimm plot method to a particle whose hydrodynamic diameter was nearly a micron. This procedure has been applied to *Serratia marcescens* ($M \sim 0.7 \times 10^{11}$), *Escherichia coli* ($M \sim 1.0 \times 10^{11}$) and *Thiobacillus ferrooxidans* ($M \sim 1.6 \times 10^{11}$). However, in general, the resonances in the angular scattered intensity envelopes have to be taken into account, and indeed provide potential information about internal structure – in terms of refractive index profiles – of microorganisms, as we will now consider.

RGD AND MIE STATIC LIGHT SCATTERING REPRESENTATIONS

Refractive index profiling of microbes (in terms of, for example, average dimensions and refractive indices of concentric regions within the microbe, see *Figure 4*) is achieved by model fitting i.e., comparing the measured angular scattered intensity envelope (*Figure 5*) with a theoretical profile based on a given model, and then iterating or refining this model until adequate agreement is obtained (Wyatt, 1973). Thus this procedure differs from the Zimm/radius of gyration method which does not require any *a priori* assumed conformation (Kerker, 1969).

The RGD representations assume no change of phase or other distortions of the electric vector caused by the scattering particle: the phase differences between scattered waves from different points in a given particle are simply a function of position within that particle and not of the material of the particle (Kerker, 1969). With RGD theory, representations are normally given for vertically polarised light since for horizontal or unpolarised light an extra term involving $\cos^2\theta$ can obscure these records (Wyatt, 1968, 1973).

Even for larger microbes the RGD theory can still give a reasonable representation of the scattered intensity profiles, provided that the refractive index difference between scatterer and medium is small (an example of this situation could be a vegetative bacterial cell in aqueous suspension). A good illustration of the range of validities of RGD is given by Kerker (1969, pp 428–429). For general RGD scatterers, the form factor $P(\theta)$ can be represented by the equation:

$$P(\theta) = (1/V^2)\left|\int_V e^{i\delta} dV^2\right| \qquad (13)$$

where the integral is over the total volume, V of a particle whose volume elements produce a scattered phase δ at a common plane.

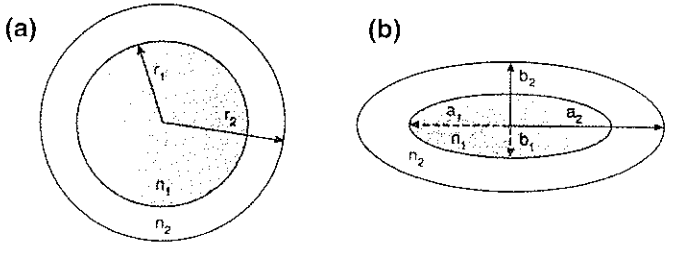

Figure 4. Refractive index profiling. **(a)** Coated sphere model: characterised by inner (or core) and outer (shell) radii r_1, r_2 and inner and outer refractive indices, n_1, n_2 respectively; **(b)** Coated ellipsoid model: inner semi-axes a_1, b_1; outer semi-axes a_2, b_2.

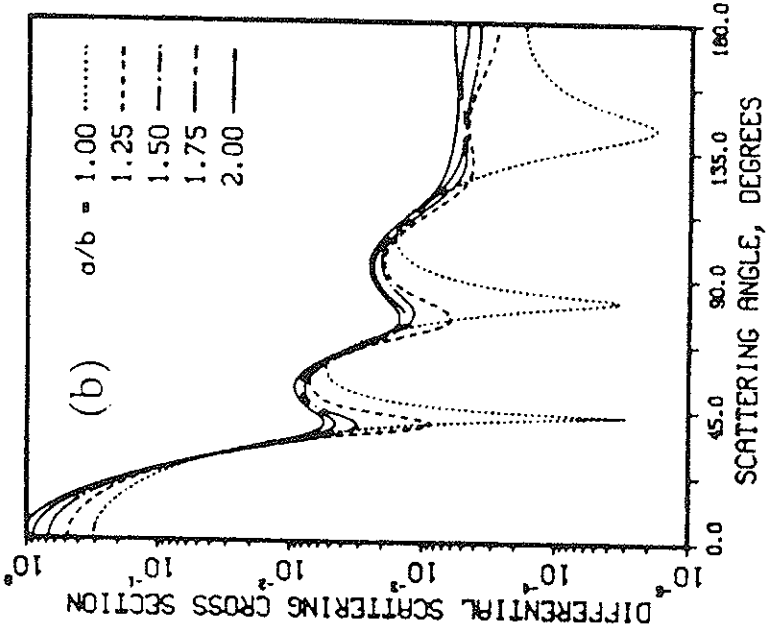
(b)
a/b = 1.00
1.25
1.50
1.75
2.00
DIFFERENTIAL SCATTERING CROSS SECTION
SCATTERING ANGLE, DEGREES
0.0
45.0
90.0
135.0
180.0

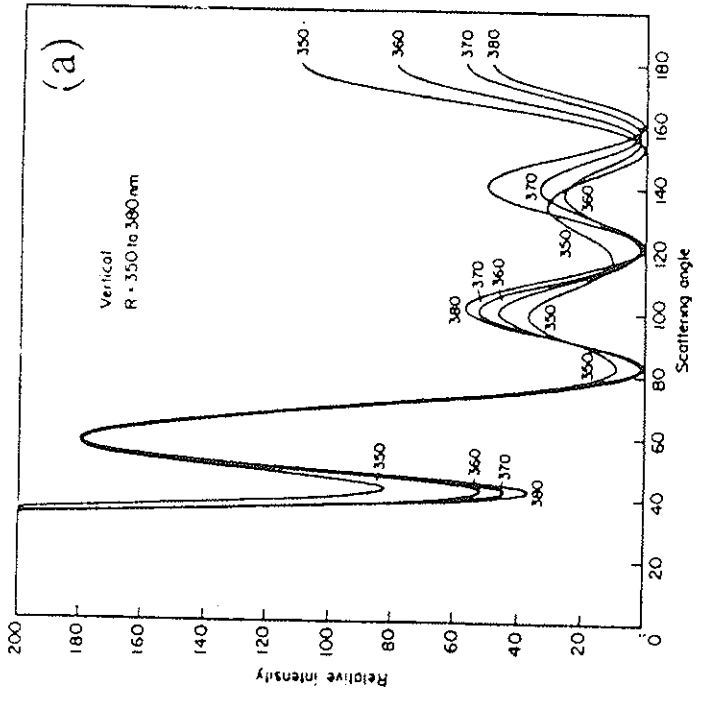
(a)
Vertical
R = 350 to 380 nm
Relative intensity
Scattering angle
350
360
370
380

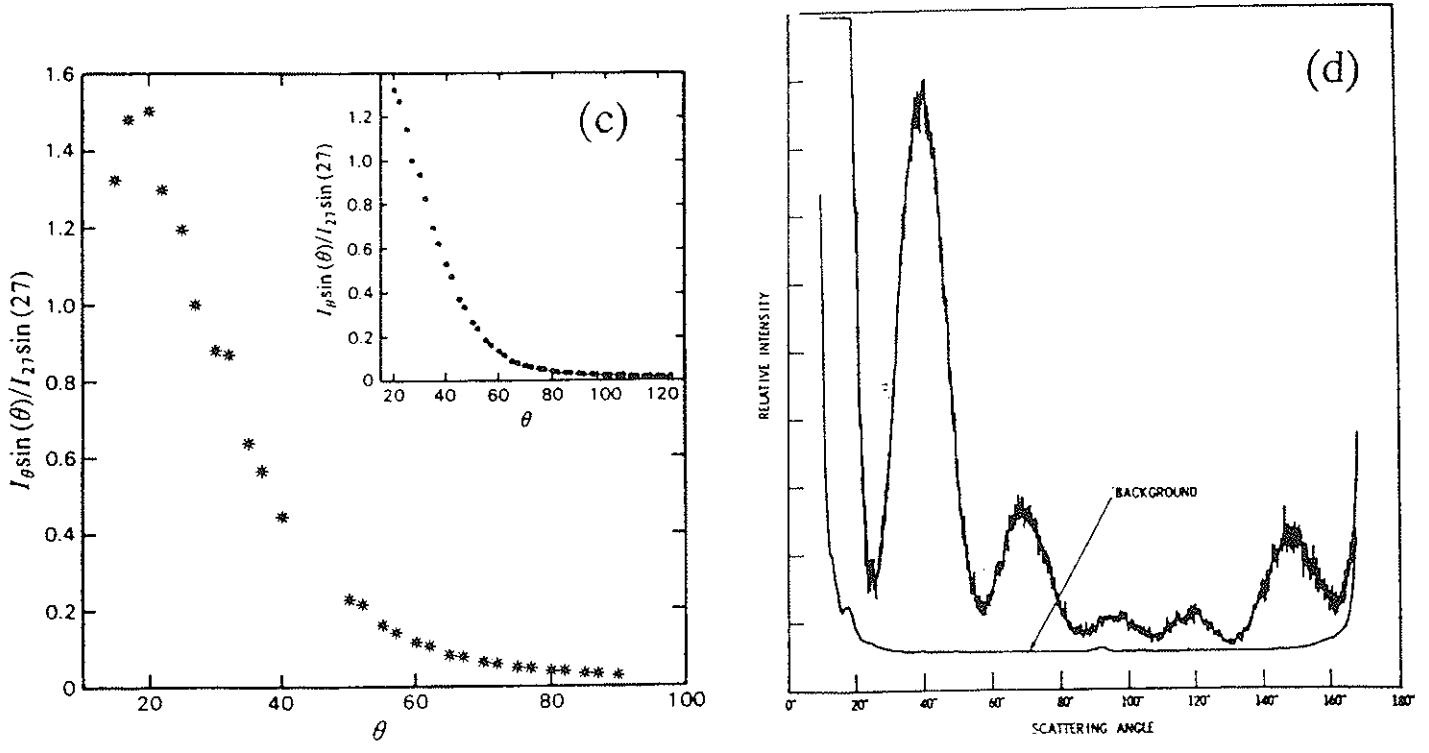

Figure 5. Angular scattered intensity envelopes from bacterial systems (vertically polarised incident radiation): **(a)** Theoretical static light scattering patterns for coated sphere models with varying radii. (Reprinted, with permission, from Wyatt 1973.) **(b)** Theoretical static light scattering for randomly oriented ellipsoidal bacteria with varying aspect ratios. The dotted line corresponds to the normalized scattering intensity function against angle for a spherical particle showing strong structural features. As the ellipsoid aspect ratio is increased the structural features in the curve are smoothed out, making modelling approaching the impossible. (Reprinted, with permission, from Wang *et al.*, 1979.) **(c)** Experimental static light scattering for a suspension of spores of *B. subtilis*. (Reprinted, with permission, from Harding and Johnson, 1984.) **(d)** Experimental static light scattering, for a single isolated spore, suspended in air, of *B. sphaericus*. (Reprinted, with permission, from Wyatt and Phillips, 1972.)

Explicit expressions for $P(\theta)$ have been worked out for a wide range of particle shape: of particular use are the concentric (two or three layered) sphere and coated ellipsoid models (*Figure 4;* Wyatt, 1968; Chen *et al.*, (1977)) for modelling the refractive indices and approximate sizes of cell nuclei, protoplasm, cytoplasm and membranes. For many microbes however – particularly for bacterial spores which have a relatively high internal refractive index – the RGD approximation is not satisfied and account has to be taken of phase changes and other distortions of the electric field caused by the scattering microbe. The theory describing such scattering behaviour (Mie) is considerably more complicated and solutions for the intensity versus angle are only available for a very limited number of particle forms. *Table 2* (Aden and Kerker, 1951; Wyatt, 1962, 1964; Asano and Sato, 1980; Barber, 1973; Barber and Massoudi, 1982; Wang *et al.*, 1979; Latimer, 1984a,b) lists those that are particularly relevant to situations involving microorganisms. For particles with spherical symmetry, the solution is summarised by the form, for vertically polarised incident light (Wyatt, 1968, 1973):

$$I(\theta) = \{Io/(qR)^2\}\left|\sum_{i=1}^{\infty}[{}^{e}B_i\tau_i(\cos\theta) + {}^{m}B_i\pi_i(\cos\theta)]\right|^2 \qquad (14)$$

where $I(\theta)$ and I_o are the intensifiers of the scattered and incident light respectively, R is the distance between the scattering particle and the reference plane or detector, ${}^{e}B_i$ and ${}^{m}B_i$ are the 'electric' and 'magnetic' scattering coefficients (involving Bessel functions) and τ_i and π_i angular functions involving Legendre type of polynomials.

Table 2. Particle types for which Lorenz-Mie solutions are available

Type	Ref
Homogeneous sphere	Mie, 1908
Coated sphere	Aden and Kerker, 1951
Multi-layered sphere	Kerker, 1969
Spheres with continuously varying refractive index	Wyatt, 1962, 1964
Homogeneous cylinders and ellipsoids	Asano and Sato, 1980
Coated ellipsoids	Barber, 1973; Barber and Massoudi, 1982; Wang *et al.*, 1979
Homogeneous spheres with holes	Latimer, 1984a
Homogeneous spheres with projections	Latimer, 1984b

ASYMMETRY AND POLYDISPERSITY

Despite the elegance of these theoretical advances, both RGD and Lorenz-Mie representations of the angular intensity envelopes have been difficult to apply for two fundamental reasons: (1) random orientations of non-spherical scatterers which tend to smooth out the resonances in the intensity envelopes. *Figure 5b* illustrates this problem for a series of coated ellipsoids which could conceivably model bacterial spores; (2) a further complication is of heterogeneity within a spore ensemble (Wyatt, 1973) and the combined effects of both asymmetry and heterogeneity can lead to rather featureless angular intensity profiles as shown in *Figure 5c* (Harding and Johnson, 1984) for an ensemble of *Bacillus subtilis* spores. It is still possible to infer

some useful information from these type of curves: for example for antibiotic susceptibility testing (Hukins *et al.*, 1980; Kielbauch *et al.*, 1989) and in studies on the marine microbe *Chlorella* (Quinby-Hunt *et al.*, 1989).

SINGLE PARTICLE MEASUREMENTS

There are two 'simple' solutions – at least in principle – to such asymmetry and heterogeneity problems. The first is to work with *quasi-spherical* bacterial spores. Although this greatly restricts the numbers of interesting systems that can be usefully analysed there are some spores – such as from *B. sphaericus* – which have reasonable spherical symmetry. The second is to record scattering intensity envelopes from isolated *single* spores. Wyatt and Phillips (1972) successfully achieved this by using an aerosol technique, giving successfully structural features which could be used for refractive index profiling (*Figure 5d*). Suspending spores in air poses additional problems, however; for example, because of the relatively large refractive index difference between microbe and air, RGD theory is almost certainly not applicable, and more seriously, the delicate osmotic balance between the interior and exterior of the microbe can be greatly disturbed – even for spores.

Instruments have been designed for multi-angle measurement (which is now referred to as 'laser diffractometry') of single particles in aqueous suspension (Ludlow and Kaye, 1979; Wyatt and Jackson, 1989). Wyatt and Jackson (1979) have indicated how such a device can be used to detect different phytoplankta from the characteristic scattered intensity envelopes. Ulanowski *et al.*, (1987; 1989) have applied coated-sphere (c.f., *Figure 4a*) Mie theory to model the refractive index profiles of spores of *B. sphaericus* and basidospores of *L. pyriforme* in water, and proposed this as a way of monitoring the water contents of spores. The technique is, however, currently limited to particles with spherical symmetry because of the random orientation problem: application to the more interesting cases of ellipsoidal spores will require ways of providing constant orientation in the incident beam for a time long enough to get a sufficient signal/noise ratio across the angular scattered intensity envelope.

FLOW CYTOMETERS

Somewhat related in principle – although primarily designed for a different purpose (counting particles) – are flow cytometers, which also facilitate light scattering measurements on single microbes (Steen and Lindmo, 1979; Salzman, 1980) and several commercial instruments are available (see, e.g., Spinrad and Brown, 1986). Light scattering detection from flow cells of suitable design are usually made at two scattering angles (Salzman, 1980): although two is too few for the modelling of internal structures, it has been inferred that data of this type can permit the identification of microbial types (Spinrad and Brown, 1986).

DYNAMIC LIGHT SCATTERING OF BACTERIAL SPORES

Dynamic light scattering can also give useful information on bacterial spores, and moreover ensembles thereof. For quasi spherical spores, the single term exponential form of the autocorrelation function (eqn6) gives a reasonable representation of the

data and as an example dynamic light scattering has been used in parallel with turbidity measurements to monitor the possible changes in the gross morphology of *B. subtilis* spores (Harding and Johnson, 1984) and *B. megaterium* spores (Harding and Johnson, 1986) during germination – particularly during the early stages.

Such information has been used to help delineate between the various theories to explain the mechanisms responsible for the strong dehydration and heat resistance of bacterial spores. A similar application has been in the use of dynamic light scattering in conjunction with electron microscopy (Molina-Garcia *et al.*, 1989) to show how culture growth temperature has an important effect on the resistance to thermal destruction (at 121°C). The effects of culture temperature on resistance to destruction by disinfectants has also been studied (Molina-Garcia *et al.*, 1989).

Chen *et al.* (1977) have shown that 'scaling' behaviour – i.e., superposition or overlap of plots of the autocorrelation function $g^{(2)}(\tau)$ plotted versus $q^2\tau$ for a range of angles – is a measure of the symmetry and homogeneity of a freely diffusing scattering particle. Non-scaling behaviour has been demonstrated for spores of *B. subtilis* (*Figure 6a*) (Harding and Johnson, 1984) and *B. megaterium* (Harding and Johnson, 1986) although *germinated* spores of *B. megaterium* do appear to scale better, possibly a measure of the decreased asymmetry and greater homogeneity of the germinated spores.

COMBINED STATIC AND DYNAMIC LIGHT SCATTERING OF SPORES

A recent study (Molina-Garcia *et al.*, 1996) used a combination of static (laser diffractometry) and dynamic light scattering on the quasi-spherical spores of *Bacillus sphaericus*, together with observations from scanning electron microscopy (*Table 3*). Dynamic light scattering, performed on a suspension of spores yielded a (z-average) Stokes radius, r_H of the spores of ~1.7, 1.6 and 1.1 μm for spores produced at 15°C, 20°C and 30°C respectively. These values are larger than those determined from laser diffractometry (0.6, 0.6 and 0.5μm) and scanning electron microscopy (0.6, 0.6 and 0.7μm). The difference reflects either aggregation or, more likely, the presence of the loose outer additional outer membrane or exosporium which affects the diffusional motion of the spores but is relatively transparent to scattering. Refractive index modelling in terms of the concentric spherical shell model (c.f., *Figure 4a*) of the laser diffractometry data also revealed an integument thickness of ~0.1μm.

Table 3. Refractive index, water content, and density of the two concentric layers of spores of *B. sphaericus* produced at different temperatures, as measured by LD. (From Molina-Garcia *et al.*, 1996.)

Spores	Refractive index		Water content (g/ml)		Density (g/ml)	
	Protoplast	Integument	Protoplast	Integument	Protoplast	Integument
BS15	1.490 ± 0.008	1.420 ± 0.006	0.38 ± 0.03	0.67 ± 0.02	1.31 ± 0.02	1.14 ± 0.01
BS20	1.480 ± 0.006	1.420 ± 0.006	0.40 ± 0.03	0.67 ± 0.02	1.29 ± 0.01	1.14 ± 0.01
BS30	1.520 ± 0.007	1.440 ± 0.008	0.26 ± 0.02	0.59 ± 0.03	1.37 ± 0.01	1.18 ± 0.01

BS15, BS20, BS30: spores produced at 15°C, 20°C and 30°C respectively.

MICROBIAL MOBILITY AND CHEMOTAXIS

This has also been a popular area. Besides being Brownian diffusers many microbes (flagellates, ciliates and bacteria) possess their own motility or 'free translational

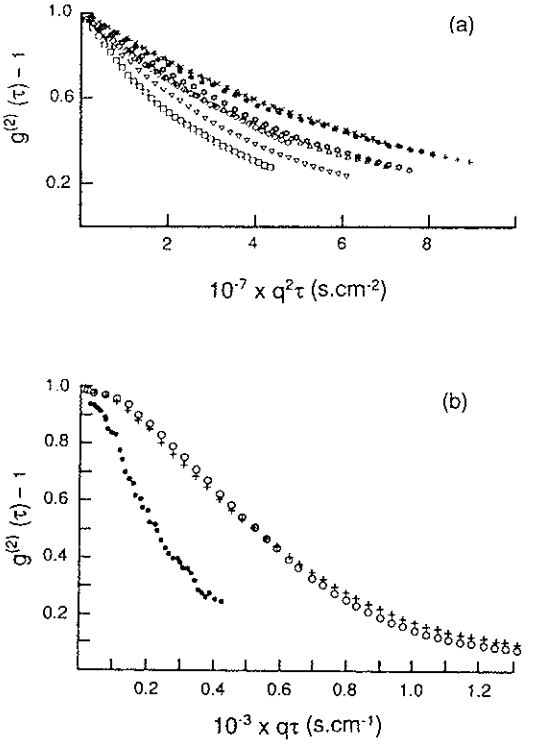

Figure 6. Dynamic light scattering scaling or 'overlap' plots of bacterial systems. (**a**) $q^2\tau$ scaling plot for spores of *Bacillus megaterium*. (From Harding and Johnson, 1986.); (**b**) $q\tau$ scaling for *E. coli*. (From Stock, 1978.). The different symbols in each case correspond to different angles. In (a) no overlap is evident. In (b) overlap is evident only at low angles.

motion' (Chen *et al.*, 1977; Nossal and Chen, 1972) deriving from their own metabolism. Dynamic light scattering has provided a powerful non-destructive and non-invasive probe into this motility to study the velocity distributions of motile bacteria such as *E. coli* (Nossal and Chen, 1972, 1973; Schaefer and Berne, 1975; Holz and Chen, 1978; Chen and Wang, 1982), *Salmonella* (Stock, 1978) and parasitic micoorganisms such as *Trypanosomas bruceii* (Gilbert *et al.*, 1983; Klein, 1984). After neglecting contributions from 'non-translational motion' (Nossal *et al.*, 1971; Stock, 1978) the general equation describing the intensity autocorrelation function $g^{(2)}(\tau)$ of motile microbes has been given as

$$[g^{(2)}(\tau) - 1]^{1/2} = \int_0^\infty [\exp(iq.V)]\, P(V)\, d^3V \qquad (15)$$

where V is the velocity and P(V) is the velocity distribution. For the relatively simple case of an isotropic distribution of velocities solution of the integral in eqn 15 gives an expression linking $g^{(2)}(\tau)$ with the root mean square velocity, the fraction of motile microorganisms and D. Scaling procedures similar to those for free Brownian diffusion (*Figure 6a*) have been developed (Wang and Chen, 1981; Chen *et al.*, 1977) involving superposition of plots of $g^{(2)}(\tau)$ versus $q\tau$ (as opposed to $q^2\tau$ for free

diffusion) for different angles as an assay for spherical symmetry and isotropicity of the scatterers. In this way, for example Stock (1978) has demonstrated scaling at low angles for *Salmonella typhimurium* (*Figure 6b*). For typical non-scalers Chen and Hallett (1982) have attempted a model to fit progressive rotational and helical movements. In more recent work Wang and Chen (1986) have studied the formation and propagation of bands of *E. coli* in the presence of oxygen and serine substrates, comparing two proposed formulisms for band formation.

References

ADEN, A.L. AND KERKER, M. (1951). *Journal of Applied Physics* **22**, 1242.

ASANO, S. AND SATO, M. (1980). *Applied Optics* **19**, 962.

BARAN, G.J. AND BLOOMFIELD, V.A. (1978). *Biopolymers* **17**, 2015.

BARBER, P.W. (1973). PhD Thesis, University of California, Los Angeles, USA.

BARBER, P.W. AND MASSOUDI, H. (1982). *Aerosol Science and Technology* **1**, 303.

BENBASAT, J.A. AND BLOOMFIELD, V.A. (1975). *Journal of Molecular Biology* **95**, 335.

BENBASAT, J.A. AND BLOOMFIELD, V.A. (1981). *Biochemistry* **20**, 5018.

BERKOWITZ, S. AND DAY, L.A. (1976). *Journal of Molecular Biology* **102**, 531.

BERTH, G., DAUTZENBERG, H., CHRISTENSEN, B.E., HARDING, S.E., ROTHER, G. AND SMIDSRØD, O (1996). *Macromolecules* **29**, 3491–3498.

BLOOMFIELD, V.A. AND LIM, T.K. (1978). In: *Methods in Enzymology* (C.H.W. Hirs and S.N. Timasheff, eds). Vol. 48 Pt. F, pp. 414–494, Academic Press, New York.

BLOOMFIELD, V.A. (1981). *Annual Reviews of Biophysics and Bioengineering* **10**, 421.

BOEDTKER, H. AND SIMMONS, N.S. (1958). *Journal of the American Chemical Society* **80**, 2550.

BRISCO, M., HANIFF, C., HULL, R., WILSON, T.M.A. AND SATTELLE, D.B. (1986). *Virology* **148**, 218.

BROWN, W. (ed) (1993). *Dynamic Light Scattering. The Method and some Applications.* Clarendon Press, Oxford UK.

BURCHARD, W. (1992). In: *Laser Light Scattering in Biochemistry* (S.E. Harding, D.B. Sattelle and V.A. Bloomfield, eds), Chapter1, Royal Society of Chemistry, Cambridge, England.

CAMERINI-OTERO, R.D. (1973). PhD thesis, New York University.

CHEN, S.-H. AND HALLETT, F.R. (1982). *Quarterly Reviews of Biophysics* **15**, 131.

CHEN, S. H. AND WANG, P.C. (1982). In: *Biomedical Applications of Laser Light Scattering* (D.B. Sattelle, W.I. Lee and B.R. Ware, eds), pp 173–190, Elsevier, Amsterdam.

CHEN, S.-H., HOLZ, M. AND TARTAGLIA, P. (1977). *Applied Optics* 16, 187.

CHERNYAK, B.V. (1982). *FEMS Microbiology Letters* **13**, 113.

COLES, H.J., JENNINGS, B.R. AND MORRIS, V.R. (1975). *Physics in Medicine and Biology* **20**, 225.

DOBOS, P., HALLETT, R., KELLS, D.T.C., SORENSEN, O. AND ROWE, D. (1977). *Journal of Virology* **22**, 150.

FIEL, R.J., MARK, E.H. AND MUNSON, B.R. (1970). *Archives of Biochemistry and Biophysics* **141**, 547.

FUJIME, S. AND MAEDA, T. (1985). *Macromolecules* **18**, 191.

GARCIA DE LA TORRE, J. (1989). In: *Dynamic Properties of Biomolecular Assemblies* (S.E. Harding and A.J. Rowe, eds), Chapter 1, Royal Society of Chemistry, Cambridge.

GARCIA DE LA TORRE, J. AND BLOOMFIELD, V.A. (1981). *Quarterly Reviews of Biophysics* **14**, 83.

GARCIA DE LA TORRE, J., CARRASCO, B. AND HARDING, S.E. (1997). *European Biophysics Journal* **28**.

GILBERT, R.J., KLEIN, R.A. AND JOHNSON, P. (1983). *Biochemical Pharmacology* **32**, 3447.

GODFREY, R.E., Johnson, P. and Stanley, C.J. (1982). In: *Biomedical Applications of Laser Light Scattering* (D.B. Sattelle, W.I. Lee and B.R. Ware, eds), pp 373–389, Elsevier, Amsterdam.

HARDING, S.E. (1986). *Biotechnology and Applied Biochemistry* **8**, 489.

HARDING, S.E. (1987). *Biophysical Journal* **51**,673.
HARDING, S.E. (1994a). *Methods in Molecular Biology* **22**, 85–95.
HARDING, S.E. (1994b). *Methods in Molecular Biology* **22**, 97–108.
HARDING, S.E. (1995). *Biophysical Chemistry* **55**, 69–93.
HARDING, S.E. AND JOHNSON, P. (1984). *Biochemical Journal* **220**, 117.
HARDING, S.E. AND JOHNSON, P. (1986). *Journal of Applied Bacteriology* **60**, 227.
HARDING, S.E. AND JOHNSON, P. (1985a). *Biochemical Journal* 231,543.
HARDING, S.E. AND JOHNSON, P. (1985b). *Biochemical Journal* 231,549.
HARDING, S.E., BERTH, G., HARTMANN, J., JUMEL, K., CÖLFEN, H. AND CHRISTENSEN, B.E. (1996). *Biopolymers* **39**, 729.
HARDING, S., HORTON, J. AND CÖLTEN, H. (1997). *European Biophysics Journal* in press.
HOLZ, M. AND CHEN, S.-H. (1978). *Applied Optics* **17**, 1930.
HOPMAN, P.C., KOOPMANS, G. AND GREVE, J. (1980). *Biopolymers* **19**, 1241.
HUKINS, D.W.L., MURRAY, J. AND EVANS, P. (1980). *UV Spectrometry Group Bulletin* **8**.
JOHNSON, P. AND BROWN, W. (1992). In: *Laser Light Scattering in Biochemistry* (S.E. Harding, D.B. Sattelle and V.A. Bloomfield eds), Chapter 11. Royal Society of Chemistry, Cambridge, England.
KERKER, M. (1969). *The Scattering of Light and other Electromagnetic Radiation*. Academic, New York.
KIEHLBAUCH, J., KENDLE, M., CARLSON, L.G., SCHEENKNECHT, F.D. AND PLORDE, J.J. (1989). *Clinics in Laboratory Medicine* 9, 319.
KLEIN, R.A. (1984). *Biochemical Society Transactions* b, 629.
LATIMER, P. (1984a). *Applied Optics* **23**, 1844.
LATIMER, P. (1984b). *Applied Optics* **23**, 442.
LUDLOW, I.K. AND KAYE, P.H. (1979). *Journal of Colloid and Interface Science* **69**, 571.
MIE, G. (1908). *Annalen der Physik* **25**, 37.
MOLINA-GARCIA, A.D. HARDING, S.E., DE PIERI, L., JAN, N. AND WAITES, W.M. (1989). *Biochemical Journal* **263**, 883.
MOLINA-GARCIA, A.D., HARDING, S.E. AND FRASER, R.S.S. (1990). *Biopolymers* **29**, 1443.
MOLINA-GARCIA, A.D., HARDING, S.E., DIAZ, F.G., GARCIA DE LA TORRE, J., ROWITCH, D. AND PERHAM, R.N. (1993). *Biophysics Journal*.
MOLINA-GARCIA, A.D., DE PIERI, L.A., LUDLOW, I., WAITES, W.M., GARCIA DE LA TORRE, J. AND HARDING, S.E. (1996). *Applied Environmental Microbiology* **62**, 1699–1704.
MORRIS, V.J., COLES, H.J. AND JENNINGS, B.R. (1974). *Nature* **249**, 240.
NIEUWENHUYSEN, P. AND CLAUWAERT, J. (1978). *Biopolymers* **17**, 2039.
NOSSAL, R. AND CHEN, S.-H. (1972). *Optics Communications* **51**, 117.
NOSSAL, R. AND CHEN, S.H. (1973). *Nature* **244**, 253.
NOSSAL, R., CHEN, S.-H. AND LAI, C.C. (1971). *Optics Communications* **4**, 35.
OLIVER, C.J., SHORTRIDGE, K.F. AND BELYAVIN, G. (1976). *Biochimica Biophysica Acta* **437**, 589.
PUSEY, P. (1974). In: *Photon Correlation and Light Beating Spectroscopy* (H.Z. Cummins and E.R. Pike, eds) pp 387–428. Plenum, New York.
QUINBY-HUNT, M.S., HUNT, A.J., LOFFTUS, K. AND SHAPIRO, D. (1989). *Limnology and Oceanography* **34**, 1587.
SAKAKI, Y., MAEDA, T. AND OSHIMA, Y. (1979). *Journal of Biochemistry (Tokyo)* **85**, 1205.
SALZMAN, G.C. (1980). In: *Cell Analysis* (N. Catsimpoolas, ed.), Chapter 5. Plenum, New York.
SANDERS, A.H. AND CANNELL, D.S. (1980). In: *Light Scattering in Liquids and Macromolecular Solutions* (V. Degiorgio, M. Corti and M. Giglio, eds), pp. 173–182. Plenum,. New York.
SANO, Y. (1987). *Journal of General Virology* **68**, 2439.
SCHAEFER, D.W. AND BERNE, B.J. (1975). *Biophysics Journal* **15**, 785.
SCHMITZ, K.S. (1990). *Dynamic Light Scattering by Macromolecules*. Academic Press, New York.
SONG, L., KIM, U.-S., WILCOXON, J. AND SCHURR, J.M. (1991). *Biopolymers* **31**, 547–567.
SPINRAD, R.W. AND BROWN, J.F. (1986). *Applied Optics* **25**, 1930.
STEEN H.B. AND LINDMO, T. (1979). *Science* **204**, 403.
STOCK, G.B. (1976). *Biophysics Journal* **16**, 535.

STOCK, G.B. (1978). *Biophysics Journal* **22**, 79.
SVEDBERG, T. AND PEDERSEN, K.O. (1940). *The Ultracentrifuge*. Oxford University Press, Oxford, UK.
TANFORD, C. (1961). *Physical Chemistry of Macromolecules* Chapter 6. Wiley and Sons, New York, 1961.
THOMAS J.C., AND FLETCHER, G.C. (1978). *Biopolymers* **17**, 2755.
TIMACHENKO, A.A., GRIKO, N.B. AND SERDYUK, I.N. (1990). *Biopolymers* **29**, 303.
ULANOWSKI, Z.J., LUDLOW, I.K. AND WAITES, M.W. (1987). FEMS *Microbiology Letters* **40**, 229.
ULANOWSKI, Z.J., LUDLOW, I.K. AND WAITES, M.W. (1989). *Microbiological Research* **93**, 28.
VAN HOLDE, K.E. (1985). *Physical Chemistry (2nd. edn)*. Chapter 4. Prentice Hall, Englewood Cliffs, New Jersey.
WANG P.C. AND CHEN, S.-H. (1981). *Biophysics Journal* **36**, 203.
WANG P.C. AND CHEN, S.-H. (1986). *Biophysics Journal* **49**,1205.
WANG, D.S., CHEN, H.C.H., BARBER, P.W. AND WYATT, P.J. (1979). *Applied Optics* **18**, 2672.
WELCH J. AND BLOOMFIELD, V.A. (1978). *Biopolymers* **17**, 2001.
WILCOXON, J. AND SCHURR, J.M. (1983). *Biopolymers* **22**, 849.
WYATT, P.J. (1962). *Physics Reviews* **127**, 1837.
WYATT, P.J. (1964). *Physics Reviews* **134**, AB1.
WYATT, P.J. (1968). *Applied Optics* **7**, 1879.
WYATT, P.J. (1992). In: *Laser Light Scattering in Biochemistry* (S.E. Harding, D.B. Sattelle and V.A. Bloomfield, eds), Chapter 3. Royal Society of Chemistry, Cambridge, England.
WYATT, P.J. (1973). *Methods in Microbiology* **8**, 183.
WYATT, P.J. AND JACKSON, C. (1989). *Limnology and Oceanography* 34, 96.
WYATT, P.J. AND PHILLIPS, D.T. (1972). *Journal of Colloid and Interface Science* **39**, 125.